The Compound LG283 Inhibits Bleomycin-induced Skin Fibrosis and Vascular Injury via Antagonizing TGF-β /Smad/Snail Mesenchymal Transition Pathways

Akira Utsunomiya
University of Fukui
Takenao Chino
University of Fukui
Natsuko Utsunomiya
University of Fukui
Vu Huy Luong
University of Fukui, Hanoi Medical University
Takashi Matsushita
Kanazawa University Graduate School of Medical Sciences: Kanazawa Daigaku Daigakuin Iyaku Hokengaku Sogo Kenkyuka Iyaku Hoken Gakuiki Igakurui
Yoko Sasaki
Link Genomics, Inc.
Dai Ogura
Link Genomics, Inc.
Shin-ichiro Niwa
Link Genomics, Inc.
Noritaka Oyama
University of Fukui
Minoru Hasegawa (minoruha@u-fukui.ac.jp)
Department of Dermatology, Division of Medicine, Faculty of Medical Sciences, University of Fukui, Japan https://orcid.org/0000-0003-3738-2682

Research article

Keywords: systemic sclerosis, fibrosis, vascular injury, therapy, mouse model, TGF-β, EMT, EndoMT, Snail

Posted Date: May 29th, 2021

DOI: https://doi.org/10.21203/rs.3.rs-529685/v1

Abstract

Background

Systemic sclerosis (SSc) is a collagen disease that exhibits intractable fibrosis and vascular injury of the skin and internal organs. Transforming growth factor-β (TGF-β)/Smad signaling plays a central role in extracellular matrix (ECM) production by myofibroblasts. Myofibroblasts may be derived from epithelial and endothelial precursor cells in addition to resident fibroblasts. Recently, our high-throughput in vitro screening discovered a small compound, LG283, that can disrupt the differentiation of dermal fibroblasts into myofibroblasts. This compound was originally generated as a curcumin derivative.

Methods

In this study, we investigated the effect of LG283 on inhibiting fibrosis and vascular injury. The action of LG283 on TGF-β-dependent fibrogenic activity, epithelial mesenchymal transition (EMT), and endothelial cell mesenchymal transition (EndoMT) was analyzed in vitro. The effects of LG283 were also examined in a bleomycin-induced skin fibrosis mouse model.

Results

LG283 suppressed TGF-β-induced ECM expression, Smad3 phosphorylation, and expression of transcription factors responsible for the mesenchymal transition, Snail 1 and 2, in cultured human dermal fibroblasts. LG283 was also found to block EMT and EndoMT in cultured human epithelial cells and endothelial cells, respectively. During these processes, Smad3 phosphorylation and/or expression of Snail 1 and 2 were inhibited by LG283 treatment. In the bleomycin-induced skin fibrosis model, oral administration of LG283 efficiently protected against the development of fibrosis and vascular injury without affecting cell infiltration or cytokine concentrations in the skin. No apparent adverse effects of LG283 were found. LG283 treatment remarkably inhibited the enhanced expression of phosphorylated Smad3 in the bleomycin-injected skin. Increased expression of Snail 1 and 2 were reduced by LG283 treatment in the mouse model.

Conclusions

The LG283 compound exhibits antagonistic activity on fibrosis and vascular injury through inhibition of TGF-β/Smad/Snail mesenchymal transition pathways and thus, may be a candidate therapeutic for treatment of SSc. Furthermore, the screening of EMT and/or EndoMT regulatory compounds may be an attractive approach for SSc therapy.

Introduction

Systemic sclerosis (SSc) is an autoimmune disease characterized by tissue fibrosis caused by excessive deposition of collagen and other extracellular matrix (ECM) components in the skin and visceral organs (1-4). Activated fibroblasts and α-smooth muscle actin (α-SMA)-positive myofibroblasts are mainly

responsible for excessive synthesis and tissue deposition of ECM in SSc. Fibroblast activation and the phenotypic transition towards myofibroblasts results from a complex series of events initiated by various pro-fibrotic molecules, including transforming growth factor-β (TGF-β), connective tissue growth factor (CTGF), platelet-derived growth factor (PDGF), and interleukin (IL)-4, IL-6, IL-13, IL-17A, and endothelin-1. Among them, TGF-β is likely the key molecule for functional activation of local fibroblasts and resultant tissue fibrosis in SSc (4, 5).

Binding of activated TGF-β to its cell surface receptor triggers intracellular signal transduction of Smad-dependent/-independent pathways. In the Smad-dependent pathway, activation of TGF-β receptor type I leads to phosphorylation of Smad2 and 3, allowing it to complex with Smad4 and translocate into the nucleus where it binds to Smad-binding element sequences of TGF-β responsive genes. Cofactors such as p300 are then recruited to the Smad-binding element-Smad complex, followed by transcriptional activation of the targeted genes. Excessive or dysregulated TGF-β/Smad signaling can result in ECM deposition and tissue fibrosis. Indeed, sustained signal activation has been detected in dermal fibroblasts of bleomycin-induced SSc mice (6) and inversely, blocking of the signaling cascade ameliorates skin fibrosis in experimental SSc models (7-11). However, no established TGF-β-targeted therapy has successfully been translated to SSc patients.

TGF-β is well known to stimulate epithelial cells to undergo epithelial mesenchymal transition (EMT) *in vitro* (12, 13). Recent reports of the close association between EMT and the establishment of SSc skin indicate; i) the epidermal basal layer of SSc skin exerts increased expression of vimentin and a Wnt gatekeeper secreted frizzled related protein 4, but inversely shows decreased expression of E-cadherin and caveolin-1 (14), ii) Twist- and Snail1-positive cells were found within eccrine glands of SSc skin (15), and iii) increased mRNA for SNAIL1, but not SNAIL2, was found in the SSc epidermis (16). Snail family zinc finger proteins are direct targets of the TGF-β cascade in epithelial cells and play a critical role in EMT during development, carcinogenesis, and tissue repair (17). Such an increase in gene expression caused by EMT-inducing transcription factors may thus promote some differentiation towards an active EMT process in the SSc epidermis.

Recently, EndoMT has also been indicated to be important in the pathogenesis of various fibrotic diseases and fibroproliferative vasculopathies including SSc (18-20). EndoMT can be induced mainly by TGF-β, although other factors, including endothelin-1, hypoxia, Wnt, Caveolin 1 and Notch, may also contribute to the process. Therefore, approaches to disrupt the process of EMT and/or EndoMT may be effective for the treatment of SSc.

Our high-throughput screening system identified LG283 from more than 1,200 compounds due to its ability to inhibit development of mesenchymal features in human dermal fibroblast cell lines. This compound was originally generated as a curcumin derivative and has been reported as a tau aggregation inhibitor by the name of PE859 (21). A previous paper demonstrated that this curcumin derivative is more effective than curcumin itself at inhibiting amyloidβ production (22). Therefore, this compound may be potentially useful for treatment of Alzheimer's disease. There are also many reports that demonstrate the

anti-fibrotic activity of curcumin via inhibition of TGF-β/Smad signaling in various organs (23). Curcumin has been reported to inhibit TGF-β/Smad signaling via suppressing degradation of the TGF-induced factor, a negative regulator of TGF-β signaling, in SSc fibroblasts (24). However, the *in vivo* effects of curcumin or its derivatives on SSc have not been demonstrated.

In this study, we show that LG283 exhibits suppressive effects on fibrosis and vascular injury in both cultured human dermal fibroblasts and in a mouse model. Our findings indicate that LG283 inhibits fibrosis and vascular injury mainly by antagonizing the TGF-β/Smad3/Snail pathway, which results in the augmentation of mesenchymal features of fibroblasts, epithelial, and endothelial cells.

Materials And Methods

LG283

LG283 was designed and synthesized as one of a series of curcumin derivatives with the original name of PE859 (3-[(1E)-2-(1*H*-indol-6-yl)ethenyl]-5-[(1E)-2-[2-methoxy-4-(2-pyridylmethoxy) phenyl] ethenyl]-1*H*-pyrazole) by Okuda and Sugimoto, et al (21).

Cell culture

Normal human dermal fibroblasts were purchased (Clontech) and were grown in Dulbecco's modified eagle medium (DMEM, Nacalai tesque) containing 10% fetal bovine serum (FBS), 100 U/ml penicillin and 100 μg/ml streptomycin (Nacalai tesque) at 37°C in a humidified 5% CO_2 atmosphere. When cells reached ~70% confluency they were starved in DMEM containing 0.1% FBS for 24 h and then pretreated with dimethyl sulfoxide (DMSO) as a control or indicated concentrations of DMSO-diluted LG283. One-hour after stimulation cells were stimulated with 10 ng/ml human recombinant (r) TGF-β1 (Peprotech) for use in experiments of immunofluorescence staining, real-time reverse transcription-polymerase chain reaction (RT-PCR), and western blot analysis. Fibroblasts between passages 3 and 5 were prepared for all experiments.

EMT

The A549 human non-small cell lung carcinoma cell line (American Type Culture Collection) was maintained in DMEM supplemented with 10% heat-inactivated FBS. Cells were seeded in 96-well plates at a density of 10,000 cells/well, 384-well plates at a density of 3,000 cells/well, and 3D-Nano-Culture Plates (SCIVAX Life Sciences). EMT was induced in DMEM containing 5% FBS with 5 ng/ml human rTGF-β2 (R&D Systems) for each indicated interval, with or without an incubation with LG283 (0.5μM) as described previously (25).

EndoMT

Normal human umbilical vein endothelial cells (HUVECs) (Kurabo Industries Ltd.) maintained in HuMedia-EG2 medium were used for EndoMT assay. Cells grown on an adhesion reagent (Kurabo Medical) to 70%

confluence were incubated with a cocktail consisting of TGF-β2 (2.5 ng/ml), TNF-α (1.0 ng/ml), and IL-1β (2.0 ng/ml) in the experimental medium (a mixture of Humedia-EG2 in serum-free RPMI, 1: 3 ratio) for each indicated interval, with or without an incubation with LG283 (0.5 μM) (26).

Animal studies

Healthy female C57BL/6 mice aged 8-10 weeks (CLEA Japan), not just siblings, were used for a bleomycin-induced skin fibrosis model (27). Bleomycin (1 mg/ml in saline) or 0.9% NaCl was injected subcutaneously into the shaved back of the mice (150 μl in each injection), concurrent with daily oral gavage of either LG283 (40 mg/kg or 80 mg/kg in sterilized olive oil) or olive oil alone for 4 weeks. The LG283 doses were optimized on the basis of sequential pilot experiments (data not shown). The drug was administered at the same time in all treatment groups for each independent experiment. All mice were housed in the same room of a specific pathogen-free barrier facility and screened regularly for pathogens.

Immunofluorescence staining

After stimulating cells with 10 ng/ml rTGF-β1 for 2 h, they were washed twice in ice-cold PBS, fixed in 100% ethanol for 10 min at room temperature, and permeabilized with 0.1% Triton X-100 in PBS for 3 min. Cells were blocked with 2% FBS for 15 min, incubated with anti-phospho-Smad3 (p-Smad3) rabbit antibody (1:50 in 2% FBS; Cell Signaling Technology) for 60 min at room temperature, and then with alexa fluor 488-conjugated goat anti-rabbit antibody for 40 min. Coverslips were mounted using Vectashield with 4',6-diamidino-2-phenylindole (DAPI, Vector Laboratories).

RT-PCR

Total RNA was isolated from the skin or cultured fibroblasts using RNeasy spin columns (Qiagen) and was digested with DNase I (Qiagen) to remove chromosomal DNA. Total RNA was reverse-transcribed to a complementary DNA with random hexamers (Takara Bio). Real-time RT-PCR was performed using the StepOnePlus Real-Time PCR system (Applied Biosystems). All data were normalized against GAPDH mRNA and are expressed as relative expression.

Western blot analysis

Total protein was extracted from human dermal fibroblasts or A549 human non-small cell lung carcinoma cell line using a 101 Bio Cytoplasmic & Nuclear Protein Extraction kit (Medibena). Samples of bleomycin-injected skin were homogenized in 600 μl of lysis buffer (10 mmoles/liter phosphate buffered saline, 0.1% SDS, 1% Nonidet P40, 5 mmoles/liter EDTA containing complete protease inhibitor mixture [Roche Diagnostics]) to extract proteins. Protein concentration was quantitated using a BCA protein assay kit (Takara Bio) on a spectrophotometer. An equal amount of protein was subjected to a standard SDS-PAGE and was transferred to a nitrocellulose membrane (Bio-Rad Laboratories Inc.). The blotted membrane was blocked for 30 min at room temperature with 5% skim milk/TBS, followed by incubation with anti-human antibodies to collagen type I alpha 2 chain (Col1A2, Abcam), fibronectin-1 (FN-1, LS bio),

phospho-Smad3 (p-Smad3, Cell Signaling Technology), SNAIL1 (Gene Tex), SNAIL2 (Invitrogen), ZEB1 (Abcam), ZEB2 (Gene Tex), Twitst 1 (Santa cruz biotechnology), GAPDH (Thermo Fisher Scientific), TUBULIN (Bio-Rad Laboratories Inc.) or anti-mouse antibodies to Smad3 (Invitrogen) , p-Smad3 (Invitrogen), GAPDH (Sigma-Aldrich) overnight at 4^{o}C. After washing with TBS-T three times, the membrane was incubated for 1 h at room temperature with HRP-conjugated secondary antibody. The protein bands were visualized using Chemi-Lumi One Super solution (Nacalai tesque). All data were normalized against GAPDH or TUBULIN expression and are expressed as relative expression.

Histologic analysis

Paraffin-embedded mouse skin sections (6 μm in thickness) were subjected to hematoxylin-eosin and Masson's trichrome staining. For evaluation of skin fibrosis, dermal thickness was defined computationally as the skin thickness from the top of the granular layers to the junction between the dermis and subcutaneous fat (28). Data were assessed in five distinct fields under an equal magnification (x 40) using a light microscope, and are expressed as mean ± SEM. Each section was examined independently by two investigators (T.C. and N.O.) in a blinded manner. Collagen deposition was quantified on Masson's trichrome-stained sections as the ratio of blue-stained area to total stained area using Adobe Photoshop Elements version 12.

Immunohistochemical staining

Paraffin-embedded mouse skin sections (6 μm in thickness) were incubated for 120 min at room temperature with monoclonal antibodies (mAbs) to CD3 (1:200; Nichirei Bioscience), F4/80 (1:100; Abcam), CD31 (1:200; Abcam), Snail1 (1:100, Gene Tex), or Snail2 (1:100; Invitrogen), then with HRP-labeled secondary antibody (Nichirei BioScience), followed by color development with the aminoethyl carbazole system (Nichirei BioScience). $CD3^{+}$ cells and $F4/80^{+}$ cells were counted under a high-power microscopic field ($CD3^{+}$ cells and $F4/80^{+}$ cells in three distinct fields). Each section was examined independently by two investigators (T.C. and N.O.) in a blinded manner. Area of the CD31-positive vessels was quantified as pixel counts in three distinct fields of each three skin sections using Adobe Photoshop Elements version 12.

Immunofluorescence staining of mouse skin

Frozen skin sections (4 μm) were fixed for 10 min in ice cold ethanol. After washing with PBS, sections were blocked by 4% Blocking ace (DS Pharma Biochemical) for 1 h at room temperature followed by incubating overnight at 4^{o}C with primary antibodies to CD31 (1:200; Abcam), F4/80 (1:100; Abcam), or Snail1 (1:100, Gene Tex). Sections were then washed with PBS and incubated with species-specific secondary antibodies for 1 hour at room temperature. Sections were mounted in VECTASHIELD mounting media containing 4', 6-diamino-2-phenylindole (Vector laboratories). Slides were visualized using laser scanning confocal microscopy (OLYMPUS FV1200).

Cytometric Bead Array

Concentrations of cytokines in skin were determined by using the Cytometric Bead Array Mouse Inflammation Kit (BD *Biosciences*). Samples (40 mg) of bleomycin-injected skin were homogenized in 600 µl of lysis buffer (10 mmoles/liter phosphate buffered saline, 0.1% SDS, 1% Nonidet P40, 5 mmoles/liter EDTA containing complete protease inhibitor mixture [Roche Diagnostics]) to extract proteins. Homogenates were centrifuged at 15,000 revolutions per minute for 15 minutes at 4 °C to remove debris, and the supernatants were used for the measurement of cytokines.

Preparation of skin cell suspensions

A 2×2.5-cm piece of depilated back skin was minced and digested in 7 ml of RPMI 1640 containing 10% FBS with 2 mg/ml crude collagenase (*Sigma-Aldrich*), 1.5 mg/ml hyaluronidase (Sigma-Aldrich), and 0.03 mg/ml DNase I (Roche Applied Science) at 37^{o}C for 90 min. Samples were passed through a 70-µm Falcon cell strainer (*BD Biosciences*) to obtain single-cell suspensions. After centrifugation at 1,500 rpm for 5 min, the cell pellet was resuspended in a 70% Percoll solution (GE Healthcare) and then overlaid with a 37% Percoll solution, followed by centrifugation at 1,800 rpm for 20 min. The cells were aspirated from the Percoll interface and passed through a 70-µm Falcon cell strainer. The harvested cells were washed with ice-cold PBS and were used for flow cytometric analysis.

Flow cytometry

mAbs used were: alexa fluor 488-conjugated anti-CD45, pacific blue-conjugated anti-CD11b, PerCP-conjugated anti-Ly6C, and APC-conjugated anti-CD204 (*R&D Systems*). To distinguish dead cells from live cells, the Live/Dead Fixable Aqua Dead Cell Stain kit (Invitrogen) was used. The single-cell suspensions obtained above were stained for 20 min at 4^{o}C using indicated mAbs at predetermined optimal concentrations for 6-color immunofluorescence analysis. Stained samples were assessed using a FACSCanto II (BD Biosciences) followed by data analysis using FlowJo software version 7 (Ashland).

Statistical analysis

All data were analyzed using Graphpad Prism software version 7 and are expressed as mean ± SEM. The significance of differences between samples was determined with Student's 2-tailed *t*-test. *P*-values less than or equal to 0.05 were considered as statistically significant. Further details are available in the Supplementary Materials and Methods.

Results

LG283 inhibits TGF-β-induced expression of ECM in human dermal fibroblasts

Excessive production of ECM by skin fibroblasts or myofibroblasts contributes to skin fibrosis. Therefore, we examined the biological effects of LG283, a small compound that was detected as a candidate for antifibrotic drug by our high-throughput *in vitro* screening, on ECM synthesis by cultured human normal skin fibroblasts. As assessed by real time-RT-PCR, baseline mRNA expression of COL1A2 and FN-1 was

significantly increased by subsequent treatment with rTGF-β1 (**Fig. 1a**). In contrast, one-hour pretreatment with 4.5 μM of LG283 significantly suppressed the TGF-β1-dependent induction of both mRNAs to steady-state levels. A similar trend was observed for the protein expression of COL1A2 and FN-1, as assessed by western blotting (**Fig. 1b**). These findings suggest that pretreatment with LG283 efficiently inhibits TGF-β-induced fibrogenic activity of skin fibroblasts.

LG283 inhibits the TGF-β-dependent increase of transcription factors responsible for the mesenchymal transition of human dermal fibroblasts

The differentiation of fibroblasts into myofibroblasts is critical for local ECM production and resultant fibrosis in the skin. Therefore, we investigated the expression of representative transcription factors responsible for the differentiation into myofibroblasts in cultured, human normal skin fibroblasts (**Fig. 1c**). The mRNA expression of zinc-finger transcriptional regulators SNAIL1 and SNAIL2 was found to increase following treatment with rTGF-β1. However, pretreatment with LG283 significantly inhibited the TGF-β-dependent induction of both mRNAs. On the other hand, rTGF-β1 and/or LG283 did not alter the expression levels of ZEB1 and ZEB2, other zinc-finger transcriptional regulators associated with the transition into myofibroblasts, suggesting LG283 specifically inhibits the TGF-β-dependent mesenchymal transition cascade.

LG283 abrogates TGF-β-dependent phosphorylation of Smad3 in human dermal fibroblasts

The TGF-β binding to its receptor induces the phosphorylation of Smad2/3 transcription factors upon canonical signaling. Phosphorylated Smad2/3 and cytoplasmic Smad4 intercommunicate to transfer the signal to the nucleus and result in the transcriptional gene regulation responsible for tissue fibrosis. We investigated the effects of LG283 on Smad phosphorylation in cultured human normal skin fibroblasts. Immunocytochemical analysis revealed that treatment with rTGF-β1 increased cytoplasmic and nuclear staining for p-Smad3 (**Fig. 1d**). However, Smad3 phosphorylation was inhibited by pretreatment with LG283.

LG283 blocks TGF-β-induced EMT in cultured A549 lung epithelial cells

We performed an EMT assay using the A549 human lung carcinoma epithelial cell line. When cultured on 2-D plates, A549 cells rapidly grew to a confluent epithelioid sheet-like appearance, which was not affected by the presence of LG283 (**Fig. 2a,** *upper panels*). Morphologically, the cells appeared round with loose clusters and sparse intercellular adhesions. Upon treatment with rTGF-β2 for 72 h, the cells changed to a fibroblastic spindle shape (**Fig. 2a,** *left lower*). However, simultaneous treatment with rTGF-β2 and LG283 somewhat negated the morphological change of A549 cells (**Fig. 2a,** *right lower*). On 3-D culture, A549 cells rapidly formed colonies of various sizes similarly in the presence and absence of LG283 (**Fig. 2b,** *upper panels*). Treatment with rTGF-β2 caused the cells to spread out to form colonies and decreased the amount of intercellular adherence and size of each colony (**Fig. 2b,** *left lower*), all of which were inhibited by simultaneous treatment with LG283 (**Fig. 2b**, *right lower*).

Next, we examined whether the LG283-dependent morphological stability is linked with epithelial and mesenchymal gene expression in 3-D cultured A549 cells. Treatment with rTGF-β2 markedly reduced the expression of E-cadherin mRNA, a representative epithelial marker, but inversely increased expression of mesenchymal markers such as FN-1, α-SMA, and CTGF at 48hr (**Fig. 2c**). The altered expression pattern of epithelial and mesenchymal markers was significantly repressed by simultaneous treatment with LG283 (**Fig. 2c**). Treatment with TGF-β2 increased the expression of SNAIL1 and SNAIL2 mRNA, but not that of ZEB1 and ZEB2 (**Fig. 2c**). The increased mRNA expression of SNAIL1 and 2 was suppressed by simultaneous treatment with LG283, although other transcription factors, ZEB1 and ZEB2, did not change in their mRNA expression (**Fig. 2c**). Similarly, protein levels of SNAIL1 and 2 were increased by TGF-β2. However, the increase was reduced by simultaneous LG283 treatment (**Fig. 2d**). Protein levels of ZEB1 and 2 and TWIST1 were not significantly changed following treatment with TGF-β2 and/or LG283 at 96h (**Fig. 2d**). Western blotting exhibited the antagonizing effect of LG283 on TGF-β1-dependent p-Smad3 expression (**Fig. 2e**). Thus, LG283 significantly blocks TGF-β-induced EMT via specific inhibition of Smad3 phosphorylation and subsequent Snail signaling in epithelial cells.

LG283 suppresses EndoMT in cultured HUVEC cells

EndoMT may affect microvascular derangement and loss of functional endothelial cells leading to poor capillary bed formation, impaired angiogenesis, and chronic tissue ischemia in addition to tissue fibrosis. Indeed, endothelial dysfunction is considered a crucial factor for peripheral vessel remodeling in SSc (18, 29-31).

We used human endothelial HUVEC cells to examine the effects of LG283 in an EndoMT assay. Upon treatment with a cocktail containing rTGF-β2, TNF-α and IL-1β, the cells exhibited reduced expression of CD31 mRNA, a representative endothelial marker, and increased expression of FN-1 mRNA, a representative mesenchymal marker, by 24 h (**Fig. 3a**). However, simultaneous treatment with LG283 resolved the disparate mRNA expression patterns of decreased endothelial marker CD31 and increased mesenchymal marker FN-1 in response to the cytokine cocktail by 24 h and 48h, respectively (**Fig. 3a**). Next, the mRNA expression levels of EndoMT-associated transcription factors were investigated in HUVEC cells treated with the cytokine cocktail and/or LG283 for 48 hours. Expression levels of both SNAIL1 and SNAIL2 were remarkably increased following stimulation with the cytokine cocktail; however, this increase was significantly inhibited by simultaneous treatment with LG283 (**Fig. 3b**). On the other hand, the expression of ZEB1 and ZEB2 mRNAs were almost unchanged following treatment with the cytokine cocktail and/or LG283. Therefore, LG283 appears to suppress the effect of cytokines, including TGF-β-induced EndoMT, via specific inhibition of Snail signaling in endothelial cells.

LG283 inhibits the development of bleomycin-induced skin fibrosis in mice

Using a bleomycin-induced skin fibrosis mouse model, we examined the *in vivo* antifibrotic effects of LG283. Subcutaneous bleomycin injection and oral LG283 were co-administrated daily for 4 weeks. No apparent side effects including the change of body weight and activity were observed in any mice (data not shown). Histologically, skin thickness was increased more than two-fold following bleomycin

injection, which was significantly reduced by both doses (40 mg/kg and 80 mg/kg) of oral LG283 (**Fig. 4a**, *upper columns***and b**, *left*). Similarly, the Masson's trichrome-stained area was significantly reduced in bleomycin-injected skin sections from LG283 treated-mice, compared to those from mice treated with placebo (**Fig. 4a**, *lower columns* **and b**, *right*).

LG283 suppresses the reduction of capillary vessels in skin of bleomycin-treated mice

To investigate the effect of LG283 on vascular injury, capillary vessels were stained with anti-CD31 antibody in bleomycin-injected skin on day 28. Subcutaneous bleomycin injection reduced the capillary vessels (**Fig. 4c**), similar to what is seen in the skin of SSc patients. However, simultaneous administration of oral LG283 significantly suppressed this decrease in capillary vessels in the skin (**Fig. 4c**). Thus, this suggests LG283 treatment is protective against destructive vascular injury during the process of skin fibrosis.

LG283 does not affect inflammatory cell infiltration during the early-stage of bleomycin-induced skin fibrosis

Subcutaneous injection of bleomycin induces an early and transient inflammation mediated by locally infiltrating macrophages and other inflammatory cells (6). Local injection of bleomycin, but not control saline, induces increased infiltration of F4/80-positive macrophages into the dermal and subcutaneous tissues at day 7 (**Fig. 4d**). In addition, there was evident local infiltration of CD3-positive T cells in bleomycin-injected skin, but not in control skin ($p<0.05$; **Fig. 4d**). However, oral LG283 administration did not affect the infiltration of these cell subsets.

To further characterize the macrophage subset present in bleomycin-treated skin, we isolated CD11b-positve leukocytes from the lesional skin on day 21 and stained for monocyte/macrophage surface markers. As reported previously (32), proinflammatory macrophages ($CD11b^{+}Ly6C^{hi}$) and profibrotic M2 macrophages ($CD11b^{+}CD204^{+}$) were both increased in bleomycin-injected skin. Oral LG283 did not significantly reduce the infiltration of macrophage subsets (**Fig. 4e**). Thus, LG283 does not appear to significantly affect the skin inflammation induced by bleomycin injection.

LG283 does not affect proinflammatory or profibrotic cytokine production in bleomycin-injected skin

The process of early inflammation and subsequent fibrosis following subcutaneous bleomycin injection can be associated with increased production of various proinflammatory and profibrotic cytokines. In general, the concentrations of investigated cytokines, IL-2, IL-4, IL-6, IL-10, IL-17A, TNF-α and interferon (IFN) -γ, were increased in fluid from bleomycin-injected skin at day 7 (**Fig. 5a**). Among these cytokines, the concentration of IL-10, a representative regulatory cytokine, in whole extracts from bleomycin-injected skin was significantly reduced by co-administration of oral LG283. However, oral LG283 treatment did not significantly change the concentration of proinflammatory cytokines, such as IL-2, IL-6, IL-17A, TNF-α and IFN-γ, or of a profibrotic cytokine, IL-4.

LG283 antagonizes the expression of phosphorylated Smad3 in bleomycin-injected skin

TGF-β/Smad signaling has been considered to be essential for tissue fibrosis. Therefore, the effect of LG283 treatment on TGF-β/Smad signaling was evaluated in the bleomycin-injected skin at day 7. The expression of TGF-β1 mRNA in bleomycin-injected skin was not significantly affected by oral LG283 (**Fig. 5b**). Similarly, LG283 administration did not change the concentration of TGF-β1 protein in the bleomycin-injected skin extraction fluid (**Fig. 5c**). Expression levels of Smad3 protein were not affected by bleomycin and/or LG283 treatment (**Fig. 5d**). In contrast, expression of p-Smad3 protein was markedly increased in bleomycin-injected skin compared to controls, an effect that was significantly inhibited by LG283 treatment of mice (**Fig. 5d**). Thus, LG283 treatment specifically inhibits the expression of the p-Smad3 in the skin of bleomycin-induced skin fibrosis model.

LG283 suppresses Snail expression in bleomycin-injected skin

Since our *in vitro* findings indicate that LG283 inhibits both TGF-β-induced EMT and EndoMT, we examined the *in vivo* expression of transcription factors associated with EMT and/or EndoMT. Similar to what was seen *in vitro*, expression of Snail1 and Snail2 mRNAs were significantly reduced in bleomycin-injected skin following administration of oral LG283 on day 7 (**Fig. 6a**). However, expression of Zeb1, Zeb2, and Twist1 mRNAs were not significantly changed by oral LG283.

Consistent with these findings, immunohistopathology showed that the expression of Snail1 and 2 were augmented in bleomycin-injected skin on day 7. However, oral LG283 inhibited the expression of both transcription factors in epidermal keratinocytes, follicular epithelial cells, and dermal fibroblasts (**Fig. 6b**). Immunofluorescent staining revealed induction of Snail1 expression in CD31-positive endothelial cells and F4/80-positive macrophages in the dermis following bleomycin injection, an effect suppressed in mice treated with oral LG283 (**Fig. 7**). Thus, LG283 treatment specifically inhibits expression of the Snail transcription factor in skin cells, including keratinocytes and endothelial cells, following bleomycin treatment.

Discussion

In this study, we investigated the inhibitory effects of the tau aggregation inhibitor, LG283, on skin fibrosis and vascular injury both *in vitro* and *in vivo*. LG283 disrupted the TGF-β1-dependent increase of Smad3 phosphorylation, Snail1 and 2 expression, and development of major skin ECMs in cultured human skin fibroblasts. Moreover, LG283 ameliorated skin fibrosis and vascular injury in a mouse model induced by subcutaneous injection of bleomycin. The *in vivo* effects of LG283 were largely attributable to the suppression of p-Smad3 and overexpression of Snail1 and 2. However, this compound did not affect inflammatory cell infiltration or inflammatory cytokine concentration in the skin during the fibrogenic process. Our results illustrate the direct antagonistic effects of LG283 and its potential for therapeutic application for inhibition of mesenchymal differentiation and the fibrogenic response.

Dermal fibroblasts from SSc skin show constitutive phosphorylation and nuclear translocation of Smad2/3 with various levels of activated Smad signaling. Therefore, targeting the TGF-β/Smad signaling is an attractive strategy for the treatment of SSc. In the current study, we confirmed that LG283 inhibits the expression of COL1α and FN-1 in human dermal fibroblasts stimulated with TGF-β1. During the process, LG283 blocks Smad3 phosphorylation and expression of Snail 1 and 2, major downstream transcription factors specific for the mesenchymal phenotype. Thus, LG283 shows anti-fibrotic activity via suppression of TGF-β/Smad/Snail signaling in dermal fibroblasts.

Accumulating evidence indicates that profibrotic myofibroblasts may be derived from various precursors including pericytes, bone marrow-derived circulating cells, epithelial cells, endothelial cells, and adipocytes (33-35). In addition, EndoMT has been considered to be possibly important for the development of fibroproliferative and/or destructive vasculopathy and thereby may link the development of endothelial dysfunction/loss and skin fibrosis in SSc (18, 35). In this study, LG283 showed *in vitro* suppressive effects on EMT of human lung epithelial cells and EndoMT of human umbilical endothelial cells induced by TGF-β2 and a cytokine cocktail (TGF-β2, TNF-α, IL-1β), respectively. Additionally, LG283 inhibited the expression of p-Smad3 in lung epithelial cells stimulated with TGF-β2. Among various cytokine-transcriptional cascades involved in the process of EMT and EndoMT, Snail1 and 2 are dominant downstream transcription factors of TGF-β/Smad signaling and are likely to play central roles. LG283 significantly inhibited the expression of both Snail 1 and Snail 2. Moreover, TGF-β1 stimulation did not increase the expression of Zeb 1 or 2, and the expression levels of these genes were not affected by LG283 treatment suggesting the mechanism is specific. These findings indicate that LG283 may antagonize Smad3 phosphorylation downstream of TGF-β as well as the subsequent upregulation of Snail1 and 2 in fibroblasts, epithelial cells, and endothelial cells during the fibrotic process.

Consistent with these *in vitro* findings, oral LG283 administration was also effective against skin fibrosis and destructive vascular injury in a bleomycin-induced skin fibrosis mouse model. In this model, skin fibrosis is preceded by an increase of inflammatory cell infiltration and inflammatory cytokine expression(36). However, LG283 did not affect the infiltration of CD3-positive T cells and macrophage subsets, including $Ly6C^{hi}$ proinflammatory and $CD204^{+}$ profibrotic macrophages, or the concentration of proinflammatory cytokines, including IL-2, IL-6, IL-17A , IFN-γ, tumor necrosis factor (TNF) -α, and profibrotic cytokine IL-4, in the inflammatory stage of bleomycin-injected skin. Therefore, the major anti-fibrotic effects of LG283 in bleomycin-injected skin do not appear to be mediated via suppression of inflammatory cell infiltration or subsequent cytokine production.

Since TGF-β/Smad3 signaling has been considered to contribute to the development of bleomycin-induced skin fibrosis (8-11, 37, 38), we evaluated the effect of LG283 on this signaling cascade. Although LG283 did not affect the expression of TGF-β1, increased expression of p-Smad3 was significantly inhibited by LG283 treatment in the bleomycin-injected skin. Interestingly, the expression of Snail1 and/or 2 was increased in skin cells including epidermal keratinocytes, endothelial cells, and macrophages following bleomycin injection, an effect inhibited by LG283 treatment. These findings were similar to that of *in vitro* investigation of TGF-β-stimulated fibroblasts and epithelial cells, and cytokine cocktail (TGF-β2,

TNF-α, IL-1β)-stimulated endothelial cells. Therefore, our findings indicate that disrupted TGF-β/Smad/Snail signaling may ameliorate skin fibrosis and vascular injury via antagonizing the differentiation of resident fibroblasts, epithelial cells, and endothelial cells into myofibroblasts.

A few points remain unclear and future studies will be required to address these issues. The effects of LG283 on skin fibrosis have only been studied in one animal model. Additionally, the anti-fibrotic and anti-vasculopathic effects of LG283 in other organs will need to be investigated in animal models. Regarding *in vitro* experiments, the effects of LG283 on EMT and EndoMT should also be confirmed in other epithelial and endothelial cell lines. Thus, additional preclinical investigations will be required and the more precise safety profile of this compound will be needed to determined prior to use of LG283 in SSc clinical trials.

Conclusions

This study demonstrates that the small compound LG283 may be effective for treatment of skin fibrotic disorders via inhibition of Smad3 phosphorylation and consequent Snail1 and 2 expression downstream of the TGF-β receptor. As a result, the differentiation of various precursors into myofibroblasts and subsequent tissue fibrosis and/or vascular injury are inhibited (**Fig. 8**). We propose that the screening of EMT and/or EndoMT regulatory compounds may result in additional therapeutic approaches for SSc treatment.

Abbreviations

SSc: systemic sclerosis; TGF: Transforming growth factor; ECM: extracellular matrix; α-SMA: α-smooth muscle actin; EMT: epithelial mesenchymal transition; EndoMT: endothelial cell mesenchymal transition; CTGF: connective tissue growth factor; PDGF: platelet-derived growth factor; IL: interleukin; DMSO: dimethyl sulfoxide; RT-PCR: real-time reverse transcription-polymerase chain reaction; GAPDH: glyceraldehyde-3-phosphate dehydrogenase; DMEM: Dulbecco's modified eagle medium; HUVECs: human umbilical vein endothelial cells; p-Smad3: phospho-Smad3; Col1A2: collagen type I alpha 2 chain; FN-1: fibronectin-1; DAPI: 4',6-diamidino-2-phenylindole; TNF: tumor necrosis factor; IFN: interferon

Declarations

Ethical Approval and Consent to participate

The animal protocols of this study were approved by the Committee on Animal Experimentation of University of Fukui (Number 29048).

Consent for publication

Not applicable.

Availability of data and materials

The datasets used and/or examined for the current study will be available from the corresponding author on reasonable request.

Competing interests

The authors declare that they have no competing interests.

Funding
This work was supported by grants from KAKENHI Grant numbers 19K08769 (to M. Hasegawa), the Japan Intractable Diseases Research Foundation (to M. Hasegawa), Research Grants from the University of Fukui (to A Utsunomiya), and Research Grants from Japan Foundation for Applied Enzymology (to A Utsunomiya).

Authors' contributions
All authors have critically reviewed and approved the final manuscript to be published. AU and MH took responsibility for the integrity of the data and the accuracy of the data analysis. Study conception and design: AU, SN, and MH. Acquisition of data: AU, TC, NU, VHL, TM, YS, and DO. Analysis and interpretation of data: AU, TC, NO, and MH.

Acknowledgements

We would like to thank Drs. Hachiro Sugimoto and Michiaki Okuda for their kind offer of the compound LG283/PE859. We thank Tomomi Shimizu and Asuka Matsuura for technical assistance.

Authors' information

[1]Department of Dermatology, Division of Medicine, Faculty of Medical Sciences, University of Fukui, Japan, [2] Department of Dermatology, Hanoi Medical University, Hanoi, Vietnam, [3]Department of Dermatology, Faculty of Medicine, Institute of Medical, Pharmaceutical and Health Sciences, Kanazawa University, Japan , [4]Link Genomics, Inc., Japan

References

1. Allanore Y, Simms R, Distler O, Trojanowska M, Pope J, Denton CP, et al. Systemic sclerosis. Nat Rev Dis Primers. 2015;1:15002.
2. Asano Y, Bujor AM, Trojanowska M. The impact of Fli1 deficiency on the pathogenesis of systemic sclerosis. J Dermatol Sci. 2010;59(3):153-62.
3. Distler JHW, Gyorfi AH, Ramanujam M, Whitfield ML, Konigshoff M, Lafyatis R. Shared and distinct mechanisms of fibrosis. Nat Rev Rheumatol. 2019;15(12):705-30.
4. Varga J, Pasche B. Antitransforming growth factor-beta therapy in fibrosis: recent progress and implications for systemic sclerosis. Curr Opin Rheumatol. 2008;20(6):720-8.

5. Lafyatis R. Transforming growth factor beta--at the centre of systemic sclerosis. Nat Rev Rheumatol. 2014;10(12):706-19.
6. Takagawa S, Lakos G, Mori Y, Yamamoto T, Nishioka K, Varga J. Sustained activation of fibroblast transforming growth factor-beta/Smad signaling in a murine model of scleroderma. J Invest Dermatol. 2003;121(1):41-50.
7. Lakos G, Takagawa S, Chen SJ, Ferreira AM, Han G, Masuda K, et al. Targeted disruption of TGF-beta/Smad3 signaling modulates skin fibrosis in a mouse model of scleroderma. Am J Pathol. 2004;165(1):203-17.
8. Hasegawa M, Matsushita Y, Horikawa M, Higashi K, Tomigahara Y, Kaneko H, et al. A novel inhibitor of Smad-dependent transcriptional activation suppresses tissue fibrosis in mouse models of systemic sclerosis. Arthritis Rheum. 2009;60(11):3465-75.
9. Santiago B, Gutierrez-Canas I, Dotor J, Palao G, Lasarte JJ, Ruiz J, et al. Topical application of a peptide inhibitor of transforming growth factor-beta1 ameliorates bleomycin-induced skin fibrosis. J Invest Dermatol. 2005;125(3):450-5.
10. Daniels CE, Wilkes MC, Edens M, Kottom TJ, Murphy SJ, Limper AH, et al. Imatinib mesylate inhibits the profibrogenic activity of TGF-beta and prevents bleomycin-mediated lung fibrosis. J Clin Invest. 2004;114(9):1308-16.
11. Wei J, Zhu H, Komura K, Lord G, Tomcik M, Wang W, et al. A synthetic PPAR-gamma agonist triterpenoid ameliorates experimental fibrosis: PPAR-gamma-independent suppression of fibrotic responses. Ann Rheum Dis. 2014;73(2):446-54.
12. Zavadil J, Bottinger EP. TGF-beta and epithelial-to-mesenchymal transitions. Oncogene. 2005;24(37):5764-74.
13. Wynn TA, Ramalingam TR. Mechanisms of fibrosis: therapeutic translation for fibrotic disease. Nat Med. 2012;18(7):1028-40.
14. Gillespie J, Tinazzi I, Colato C, Benedetti F, Biasi D, Caramaschi P, et al. Epithelial cells undergoing epithelial mesenchymal transition (EMT) in systemic sclerosis lack caveolin-1 and modulate WNT signaling in the dermis by secreting SFRP4. Ann Rheum Dis. 2011;70 Suppl 2(1468-2060 (Electronic)):A1-100.
15. Nakamura M, Tokura Y. Expression of SNAI1 and TWIST1 in the eccrine glands of patients with systemic sclerosis: possible involvement of epithelial-mesenchymal transition in the pathogenesis. Br J Dermatol. 2011;164(1)(1365-2133 (Electronic)):204-5.
16. Nikitorowicz-Buniak J, Denton CP, Abraham D, Stratton R. Partially Evoked Epithelial-Mesenchymal Transition (EMT) Is Associated with Increased TGFbeta Signaling within Lesional Scleroderma Skin. PLoS One. 2015;10(7):e0134092.
17. Lamouille S, Xu J, Derynck R. Molecular mechanisms of epithelial-mesenchymal transition. Nat Rev Mol Cell Biol. 2014;15(3):178-96.
18. Manetti M, Romano E, Rosa I, Guiducci S, Bellando-Randone S, De Paulis A, et al. Endothelial-to-mesenchymal transition contributes to endothelial dysfunction and dermal fibrosis in systemic

sclerosis. Ann Rheum Dis. 2017;76(5):924-34.

19. Mendoza FA, Piera-Velazquez S, Farber JL, Feghali-Bostwick C, Jimenez SA. Endothelial Cells Expressing Endothelial and Mesenchymal Cell Gene Products in Lung Tissue From Patients With Systemic Sclerosis-Associated Interstitial Lung Disease. Arthritis Rheumatol. 2016;68(1):210-7.
20. Good RB, Gilbane AJ, Trinder SL, Denton CP, Coghlan G, Abraham DJ, et al. Endothelial to Mesenchymal Transition Contributes to Endothelial Dysfunction in Pulmonary Arterial Hypertension. Am J Pathol. 2015;185(7):1850-8.
21. Okuda M, Hijikuro I, Fujita Y, Wu X, Nakayama S, Sakata Y, et al. PE859, a novel tau aggregation inhibitor, reduces aggregated tau and prevents onset and progression of neural dysfunction in vivo. PLoS One. 2015;10(2):e0117511.
22. Urano Y, Takahachi M, Higashiura R, Fujiwara H, Funamoto S, Imai S, et al. Curcumin Derivative GT863 Inhibits Amyloid-Beta Production via Inhibition of Protein N-Glycosylation. Cells. 2020;9(2).
23. Yu Y, Sun J, Wang R, Liu J, Wang P, Wang C. Curcumin Management of Myocardial Fibrosis and its Mechanisms of Action: A Review. Am J Chin Med. 2019;47(8):1675-710.
24. Song K, Peng S, Sun Z, Li H, Yang R. Curcumin suppresses TGF-beta signaling by inhibition of TGIF degradation in scleroderma fibroblasts. Biochem Biophys Res Commun. 2011;411(4):821-5.
25. Arai K, Eguchi T, Rahman MM, Sakamoto R, Masuda N, Nakatsura T, et al. A Novel High-Throughput 3D Screening System for EMT Inhibitors: A Pilot Screening Discovered the EMT Inhibitory Activity of CDK2 Inhibitor SU9516. PLoS One. 2016;11(9):e0162394.
26. Nagai T, Kanasaki M, Srivastava SP, Nakamura Y, Ishigaki Y, Kitada M, et al. N-acetyl-seryl-aspartyl-lysyl-proline inhibits diabetes-associated kidney fibrosis and endothelial-mesenchymal transition. Biomed Res Int. 2014;2014(2314-6141 (Electronic)):696475.
27. Yamamoto T, Takagawa S, Katayama I, Yamazaki K, Hamazaki Y, Shinkai H, et al. Animal model of sclerotic skin. I: Local injections of bleomycin induce sclerotic skin mimicking scleroderma. J Invest Dermatol. 1999;112(4):456-62.
28. Tanaka C, Fujimoto M, Hamaguchi Y, Sato S, Takehara K, Hasegawa M. Inducible costimulator ligand regulates bleomycin-induced lung and skin fibrosis in a mouse model independently of the inducible costimulator/inducible costimulator ligand pathway. Arthritis Rheum. 2010;62(6):1723-32.
29. Manetti M, Guiducci S, Ibba-Manneschi L, Matucci-Cerinic M. Mechanisms in the loss of capillaries in systemic sclerosis: angiogenesis versus vasculogenesis. J Cell Mol Med. 2010;14(6A):1241-54.
30. Manetti M Fau - Guiducci S, Guiducci S Fau - Matucci-Cerinic M, Matucci-Cerinic M. The origin of the myofibroblast in fibroproliferative vasculopathy: does the endothelial cell steer the pathophysiology of systemic sclerosis? Arthritis Rheum. 2011;63(8)(1529-0131 (Electronic)):2164-7.
31. Matucci-Cerinic M, Kahaleh B, Wigley FM. Review: Evidence That Systemic Sclerosis Is a Vascular Disease. Arthritis and Rheumatism. 2013;65(8):1953-62.
32. Luong VH, Chino T, Oyama N, Matsushita T, Sasaki Y, Ogura D, et al. Blockade of TGF-beta/Smad signaling by the small compound HPH-15 ameliorates experimental skin fibrosis. Arthritis Res Ther. 2018;20(1):46.

33. Ebmeier S, Horsley V. Origin of fibrosing cells in systemic sclerosis. Curr Opin Rheumatol. 2015;27(6):555-62.
34. Marangoni RG, Korman BD, Wei J, Wood TA, Graham LV, Whitfield ML, et al. Myofibroblasts in murine cutaneous fibrosis originate from adiponectin-positive intradermal progenitors. Arthritis Rheumatol. 2015;67(4):1062-73.
35. Piera-Velazquez S, Li Z, Jimenez SA. Role of endothelial-mesenchymal transition (EndoMT) in the pathogenesis of fibrotic disorders. Am J Pathol. 2011;179(3):1074-80.
36. Yoshizaki A, Yanaba K, Yoshizaki A, Iwata Y, Komura K, Ogawa F, et al. Treatment with rapamycin prevents fibrosis in tight-skin and bleomycin-induced mouse models of systemic sclerosis. Arthritis Rheum. 2010;62(8):2476-87.
37. Distler JH, Jungel A, Huber LC, Schulze-Horsel U, Zwerina J, Gay RE, et al. Imatinib mesylate reduces production of extracellular matrix and prevents development of experimental dermal fibrosis. Arthritis Rheum. 2007;56(1):311-22.
38. Ruzehaji N, Frantz C, Ponsoye M, Avouac J, Pezet S, Guilbert T, et al. Pan PPAR agonist IVA337 is effective in prevention and treatment of experimental skin fibrosis. Ann Rheum Dis. 2016;75(12):2175-83.

Figures

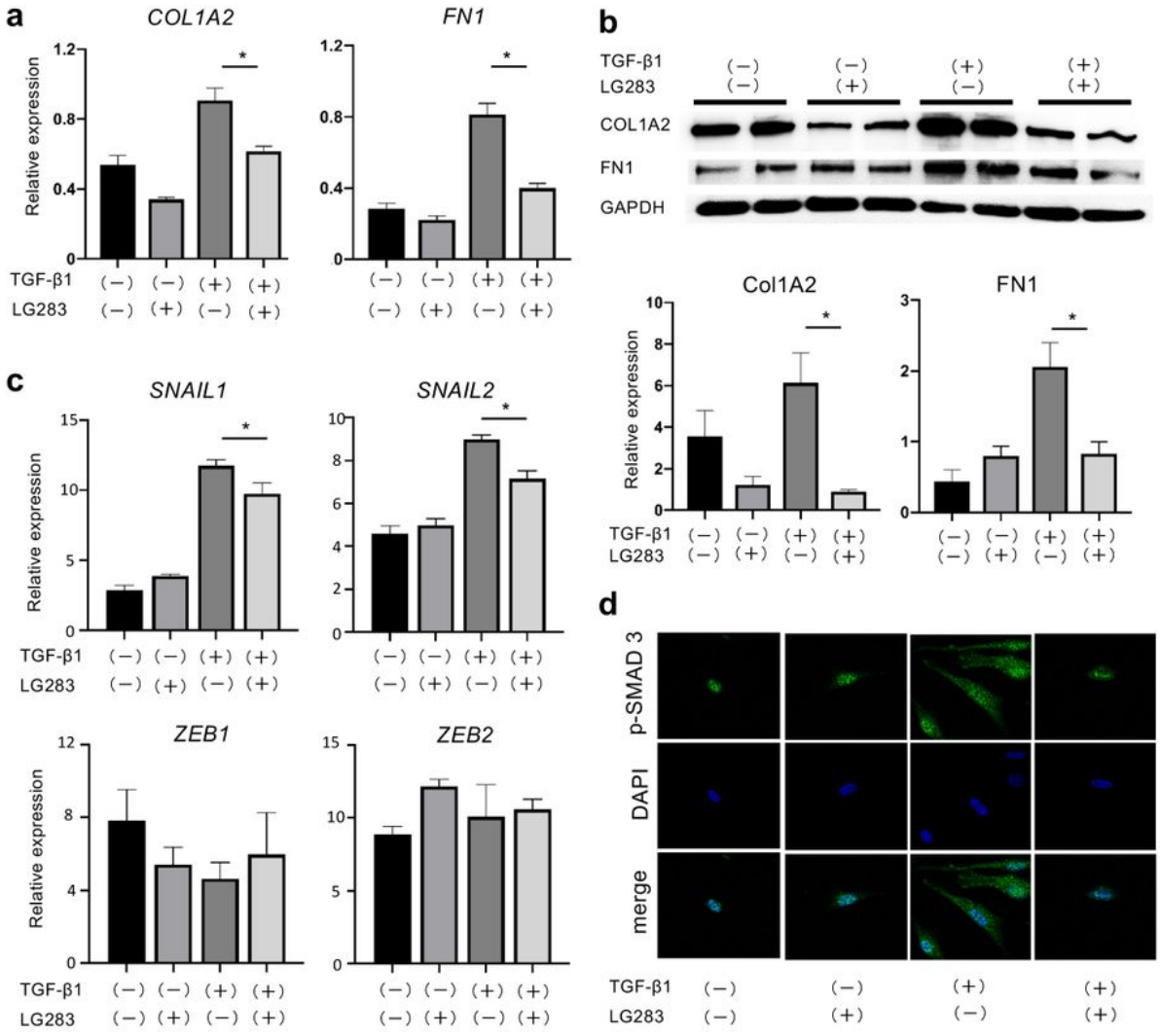

Figure 1

LG283 inhibits the fibrogenic activity of cultured human dermal fibroblasts stimulated with TGF-β1. Human fibroblasts were pretreated with DMSO or various concentrations of DMSO-diluted LG283 for 1 hour, followed by stimulation with 10 ng/ml human rTGF-β1 for additional 24 h. (a and b) After harvest, mRNA and protein expression of COL1A2 and FN-1 were evaluated by real-time RT-PCR and western blot, respectively. Values were normalized to GAPDH levels and are shown as the mean of fold change

compared to vehicle control ± SEM. All values represent mean ± SEM; n = 5 each group; *, p ≤ 0.05. (c) Effects of LG283 on mRNA expression of transcription factors associated with mesenchymal transition in human dermal fibroblasts. All values represent mean ± SEM; n = 5 each group; *, p ≤ 0.05. (d) Human dermal fibroblasts were immunostained for phospho Smad3 (p-Smad3, green). Representative images are shown on the left (40-fold magnification). All values represent mean ± SEM; n = 5 each group; **, p ≤ 0.01.

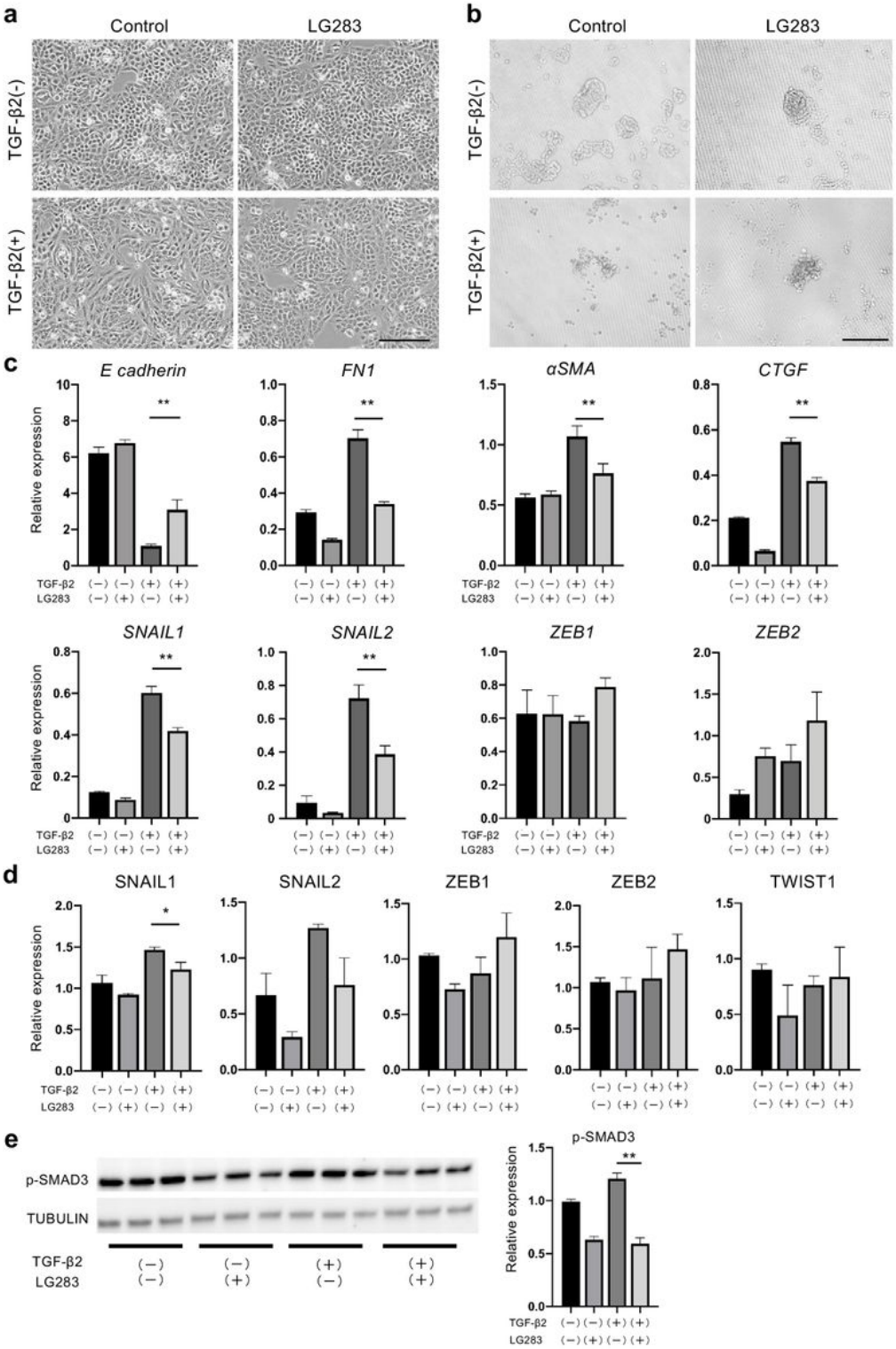

Figure 2

LG283 antagonizes EMT in vitro. The effect on EMT in NanoCulture Plate (NCP). Human lung carcinoma epithelial cell line A549 cells were grown in either 2-D or 3-D NCP conditions with or without rTGF-β2 only or TGF-β2-plus LG283. (a) Representative images of 2-D cultured A549 cells. The cells exhibited a round, confluent epithelioid appearance irrespective of the presence (right upper) or absence of LG283 (left upper). Treatment with rTGF-β2 for 72 h resulted in a morphological change to fibroblastic spindle shape (left lower), which was blocked by co-treatment with LG283 (right lower). (b) Representative images of 3-D nanocultured A549 cells. The cells rapidly colonized and grew similarly in the absence or presence of LG283 (right or left lower, respectively). Treatment with rTGF-β2 for 72 h induced decolonization with poor intercellular junction formation and decreased colony size (left lower). Both of these effects were blocked by co-treatment with LG283 (right lower). Scale bars, 200 μm. (c) mRNA expression of epithelial (E-cadherin) and mesenchymal makers (FN-1, α-SMA, CTGF) and transcription factors associated with EMT (SNAIL1, 2 and ZEB1, 2) were quantified by real-time RT-PCR at 48h. Values were normalized to GAPDH levels and are shown as the mean of fold change compared to vehicle control ± SEM of three independent experiments; n=5 each group; **, $p \leq 0.01$. (d) Protein expression of EMT-associated transcription factors were quantified by western blot analyses at 48-96h. Values were normalized to GAPDH levels and are shown as the mean of fold change compared to vehicle control; n=4 each group. All values represent mean ± SEM; *, $p \leq 0.05$. (e) After 48 h incubation of A549 cells with or without rTGF-β2 only or TGF-β2-plus LG283, protein expression of p-Smad3 were evaluated by western blot. Values were normalized to TUBLIN levels and are shown as the mean of fold change compared to vehicle control ± SEM; n=4 each group ; **, $p \leq 0.01$.

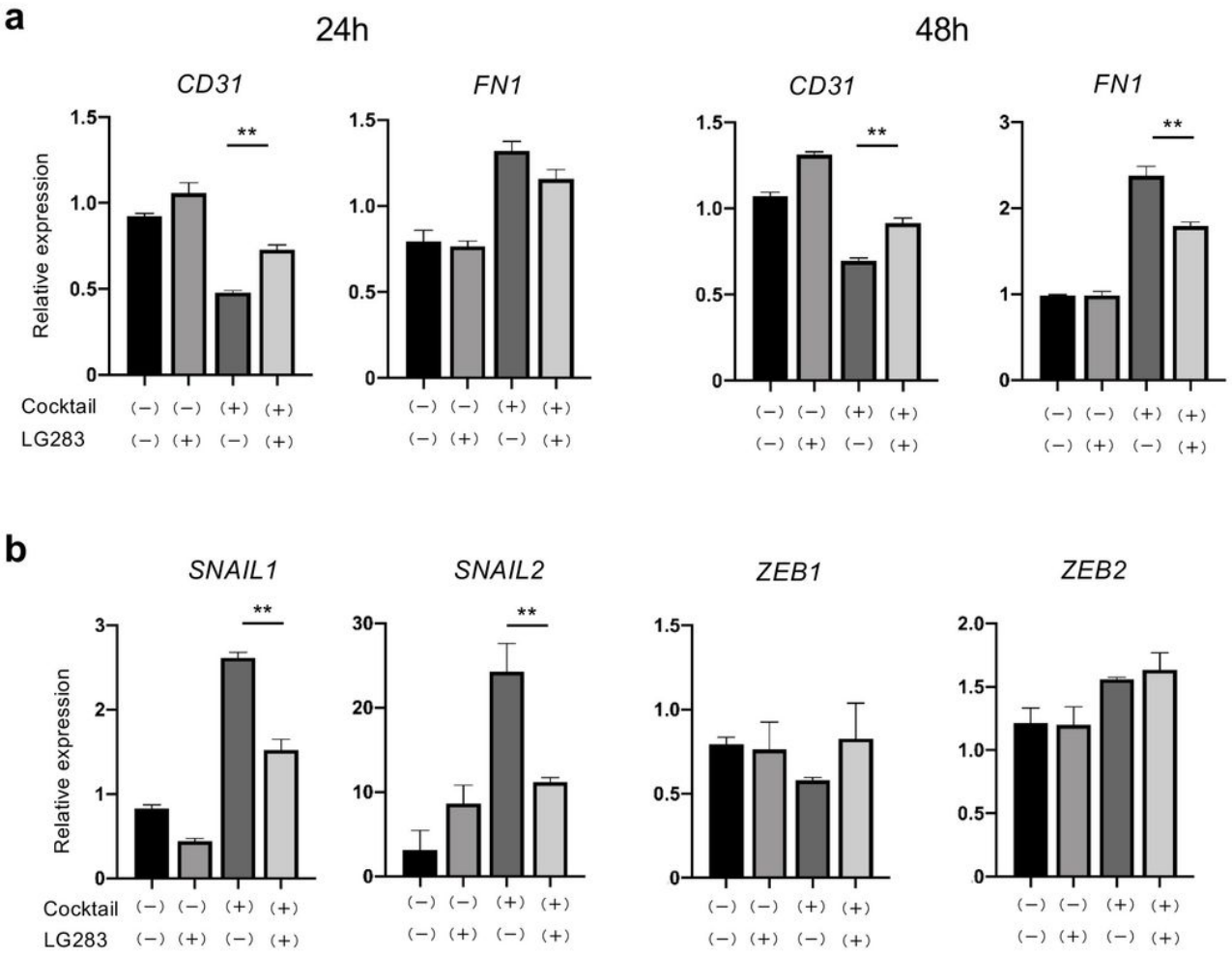

Figure 3

LG283 antagonizes EndoMT in vitro. HUVEC cells were exposed to a combination of cytokines (TGF-β2 at 2.5 ng/ml, TNF-α at 1.0 ng/ml, and IL-1β at 2.0 ng/ml) in experimental medium for the indicated interval or 48 h, in the presence or absence of LG283 (0.5 μM). Expression of an endothelial marker (CD31), mesenchymal marker (FN-1) (a), and transcription factors associated with EndoMT (SNAIL1, 2, and ZEB1, 2) (b) were quantified with real-time qRT-PCR. Values were normalized to GAPDH levels and are shown as the mean of the fold change compared to vehicle control ± SD of three independent experiments. All values represent mean ± SEM; n =4 each group; **, $p \leq 0.01$.

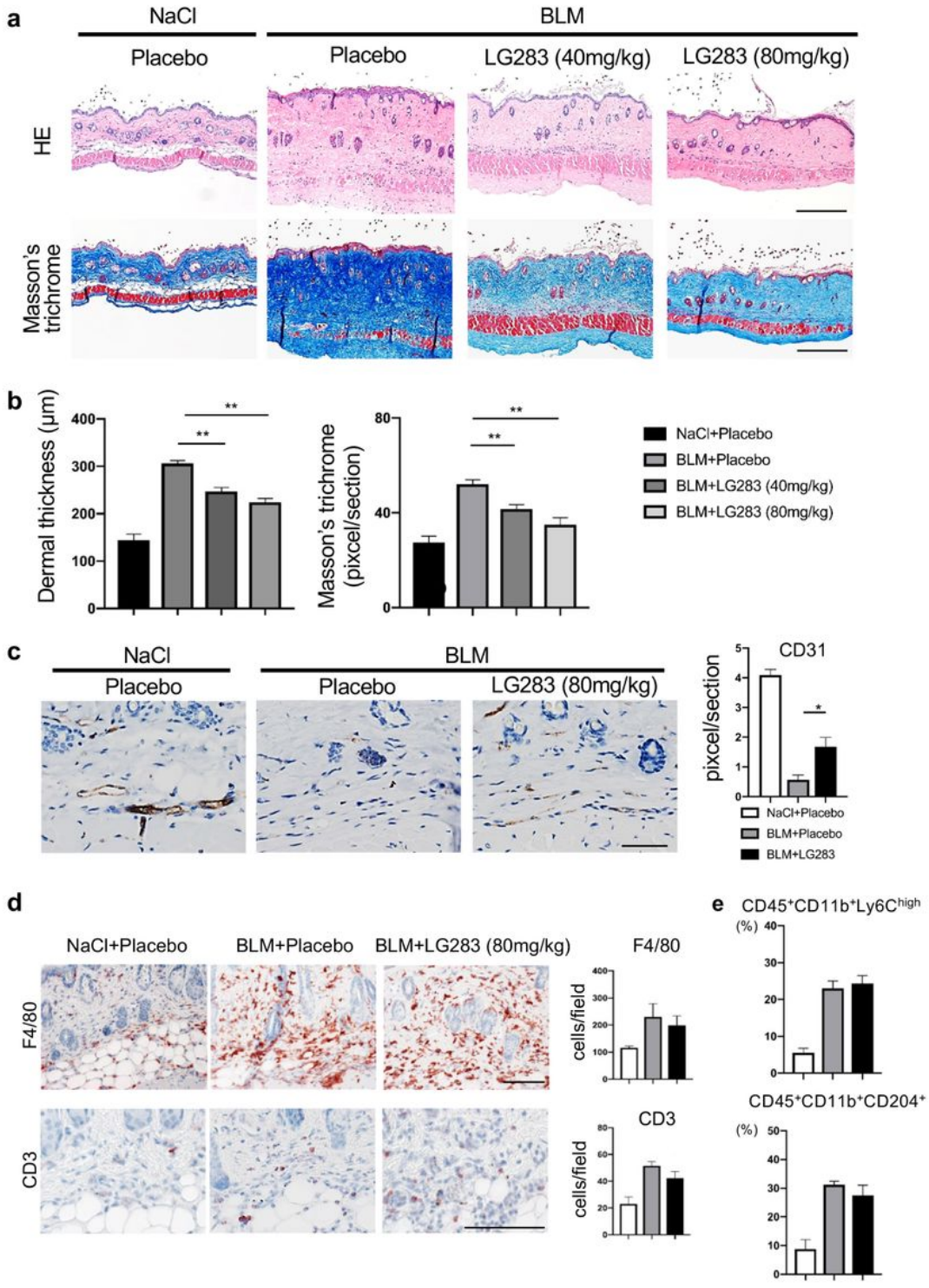

Figure 4

Oral LG283 administration ameliorates bleomycin-induced skin fibrosis regardless of inflammation in mice. (a) The antifibrotic effects of LG283 were analyzed in the back skin of mice receiving daily subcutaneous injections of bleomycin concurrent with daily oral gavage of LG283 or placebo (sterilized olive oil) for 4 weeks. Representative images of H&E stained (upper columns) and Masson's trichrome stained tissue (lower columns). Scale bar, 200 μm. (b) Skin fibrosis in bleomycin-injected mice with or

without oral LG283 was compared by determining dermal thickness and ratio of trichrome-stained area/total area. Values represent mean ± SEM; n =10 each group; **, $p \leq 0.01$. (c) Oral LG283 suppresses the bleomycin-induced decrease of dermal capillary vessels in mice. Representative immunohistochemistry images of day 28 are shown (left). Scale bar, 50 μm. Quantitative analysis is shown in the bar graph (right). Values represent mean ± SEM; n =3 each group; *, $p \leq 0.05$. (d) Oral LG283 did not affect the infiltration of F4/80-positive or CD3-positive leukocytes in the skin of mice after 7 days of daily bleomycin injections. Representative images are shown (left). Scale bar, 50 μm. Quantitative analysis is shown in the bar graph (right). Values represent mean ± SEM; n =5 each group. (e) Oral LG283 did not change the infiltration of inflammatory CD11b+Ly6Chi monocytes and profibrotic CD11b+CD204+ M2 macrophages analyzed by flow cytometry after 21 days of bleomycin injection. Values represent mean ± SEM; n = 5 each group.

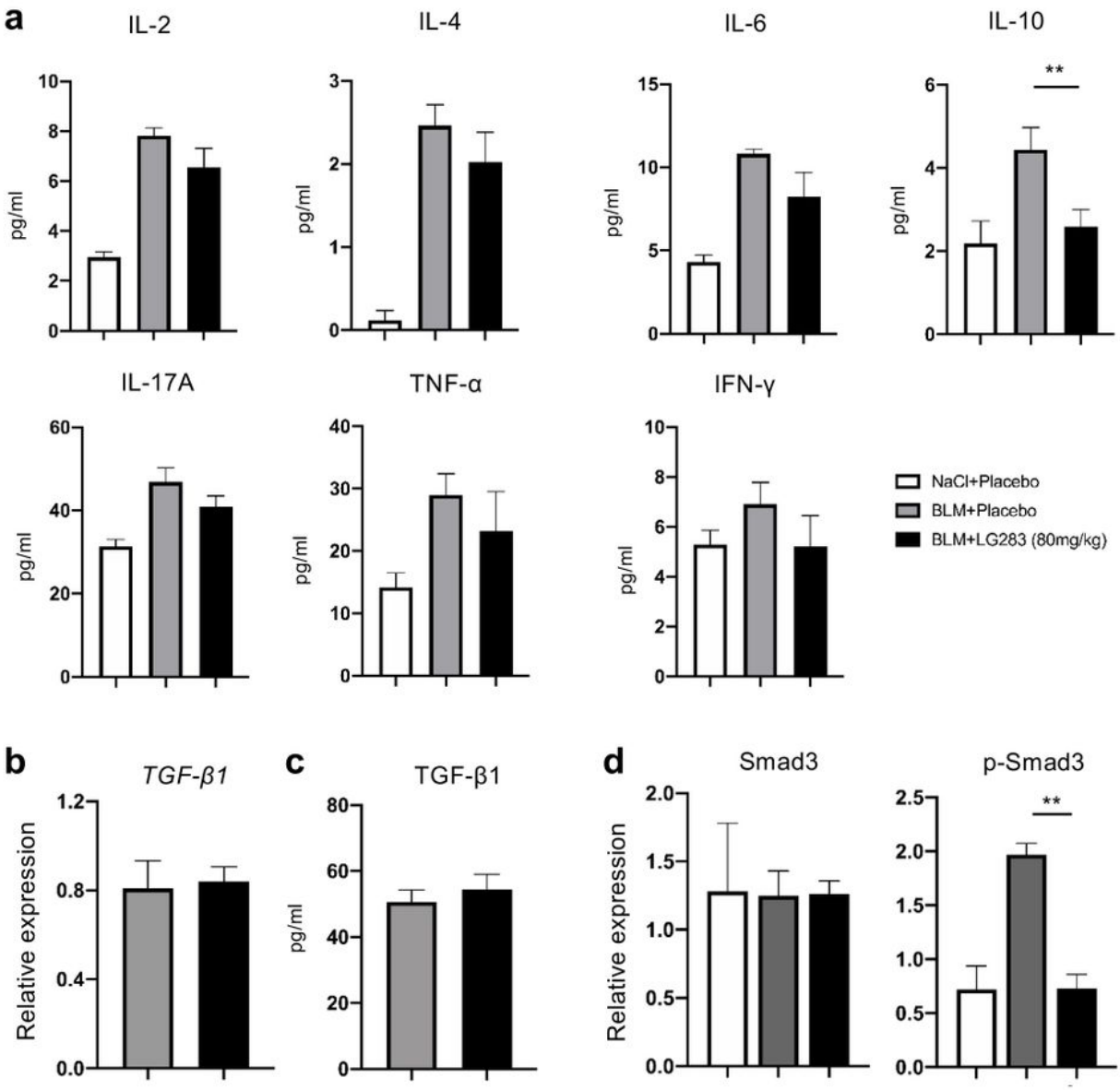

Figure 5

The effect of oral LG283 on expression of cytokines and Smad3. Crude lysate and mRNA were extracted from skin samples of placebo- and LG283-treated mice at day 7 after bleomycin injection. (a) Concentration of the indicated cytokines was examined by cytometric bead array. Values represent mean ± SEM; n=5 each group; **, p< 0.01. (b and c) TGF-β1 mRNA and protein as evaluated with real-time RT-PCR of the skin and cytometric bead array of the skin extracts, respectively. Values represent mean ±

SEM; n = 5 each group. (d) Protein expression levels of Smad3 and p-Smad3 were quantified using western blotting. Values represent mean ± SEM; n = 5 each group; **, p< 0.01.

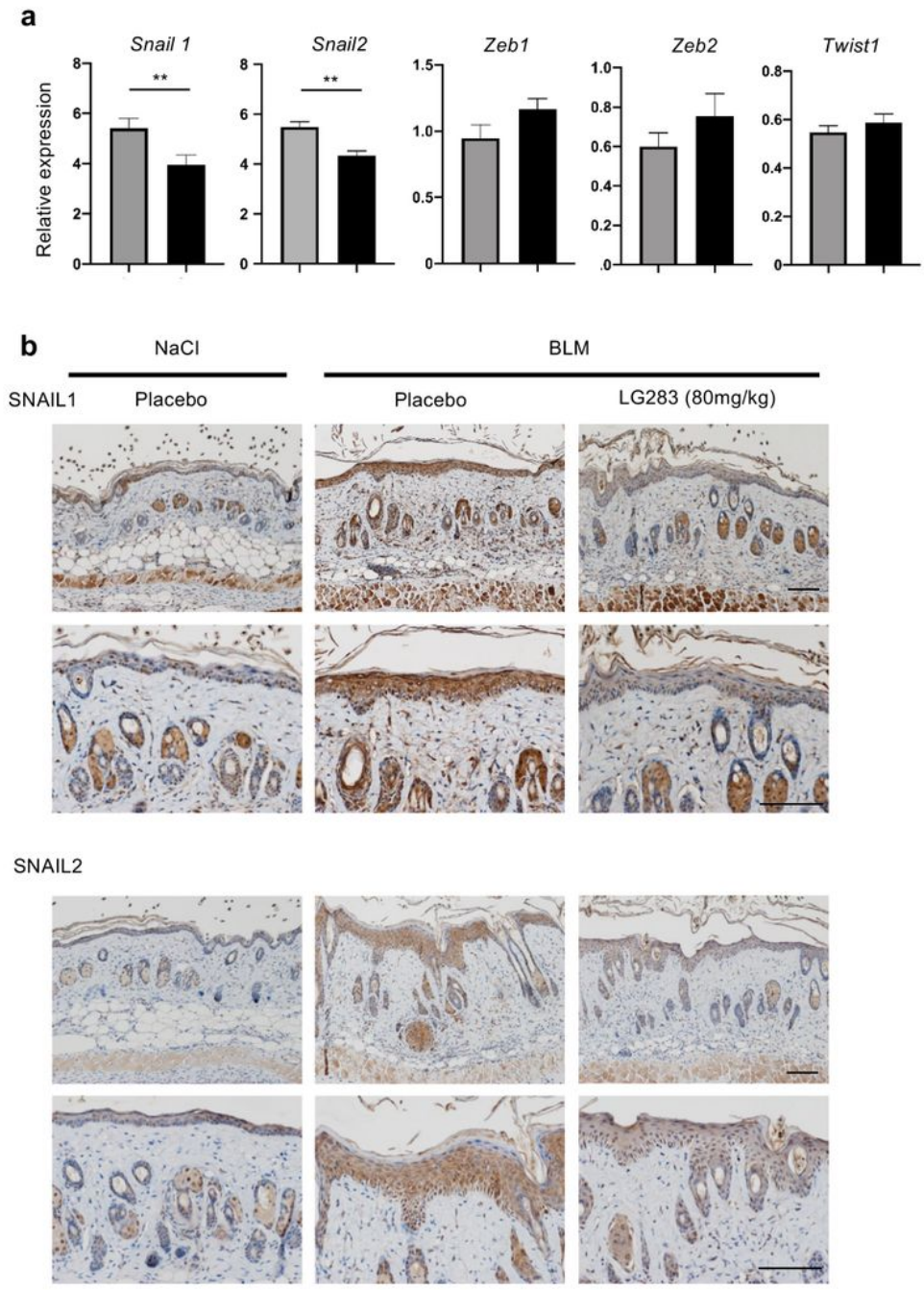

Figure 6

The effect of oral LG283 on the expression of transcription factors associated with EMT and EndoMT in bleomycin-injected mouse skin. (a) mRNA expression of transcription factors in skin samples of placebo- and LG283-treated mice at day 7 after bleomycin injection were quantitatively analyzed by real-time RT-

PCR. Values represent mean ± SEM; n = 5 each group; **, p< 0.01. (b) Skin sections were immunostained for SNAIL1 and 2. Scale bar, 100 μm. Representative immunohistochemistry images are shown. n = 5 each group.

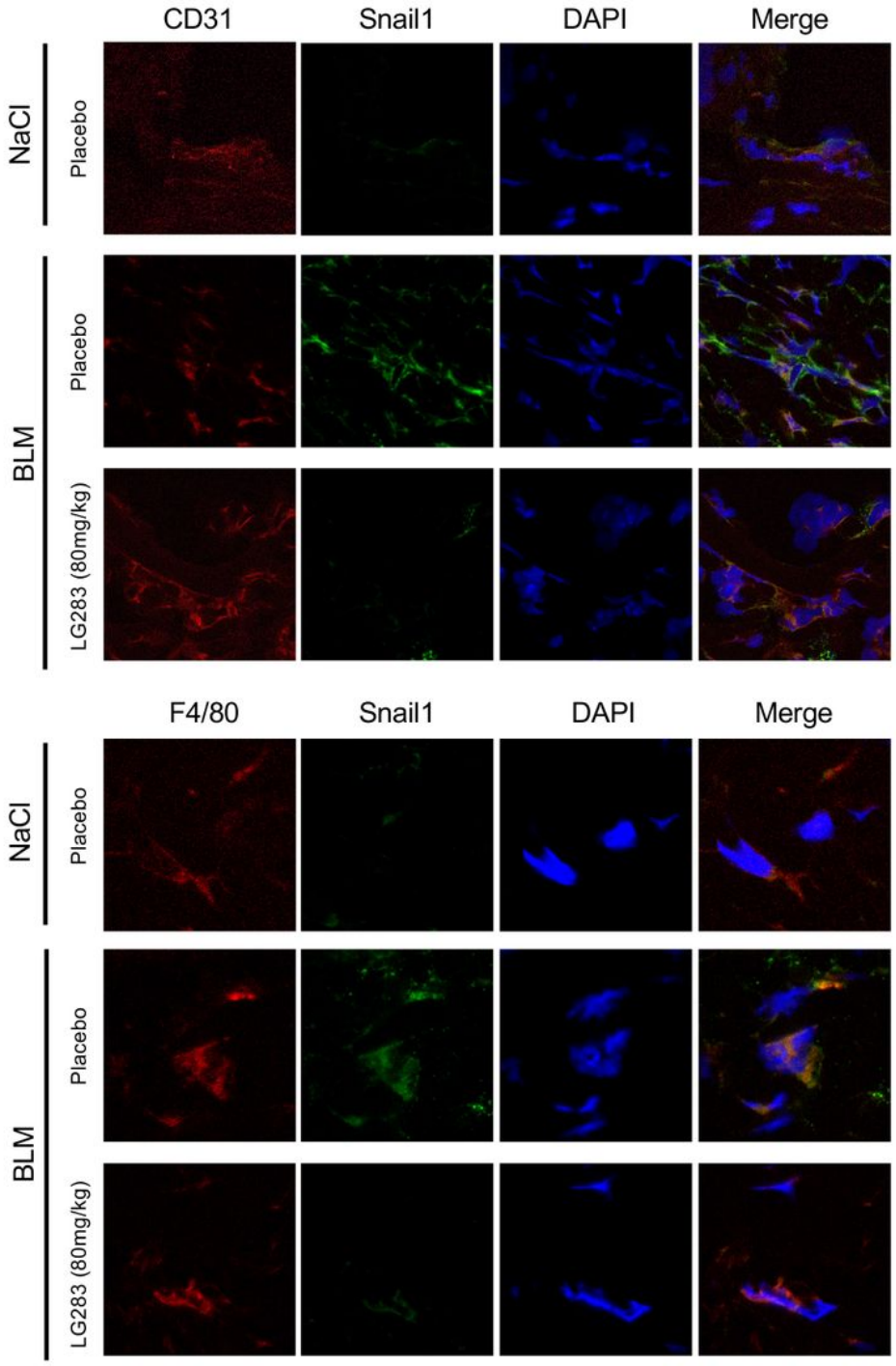

Figure 7

Snail1 expression in endothelial cells and macrophages in bleomycin-injected skin. Cryosections of the bleomycin-injected skin (day 7) were subjected to immunofluorescent staining for 4',6-diamidino-2-

phenylindole (DAPI) (blue), CD31 or F4/80 (red), and Snail1 (green). Representative immunohistochemistry images are shown (left). n =3 each group.

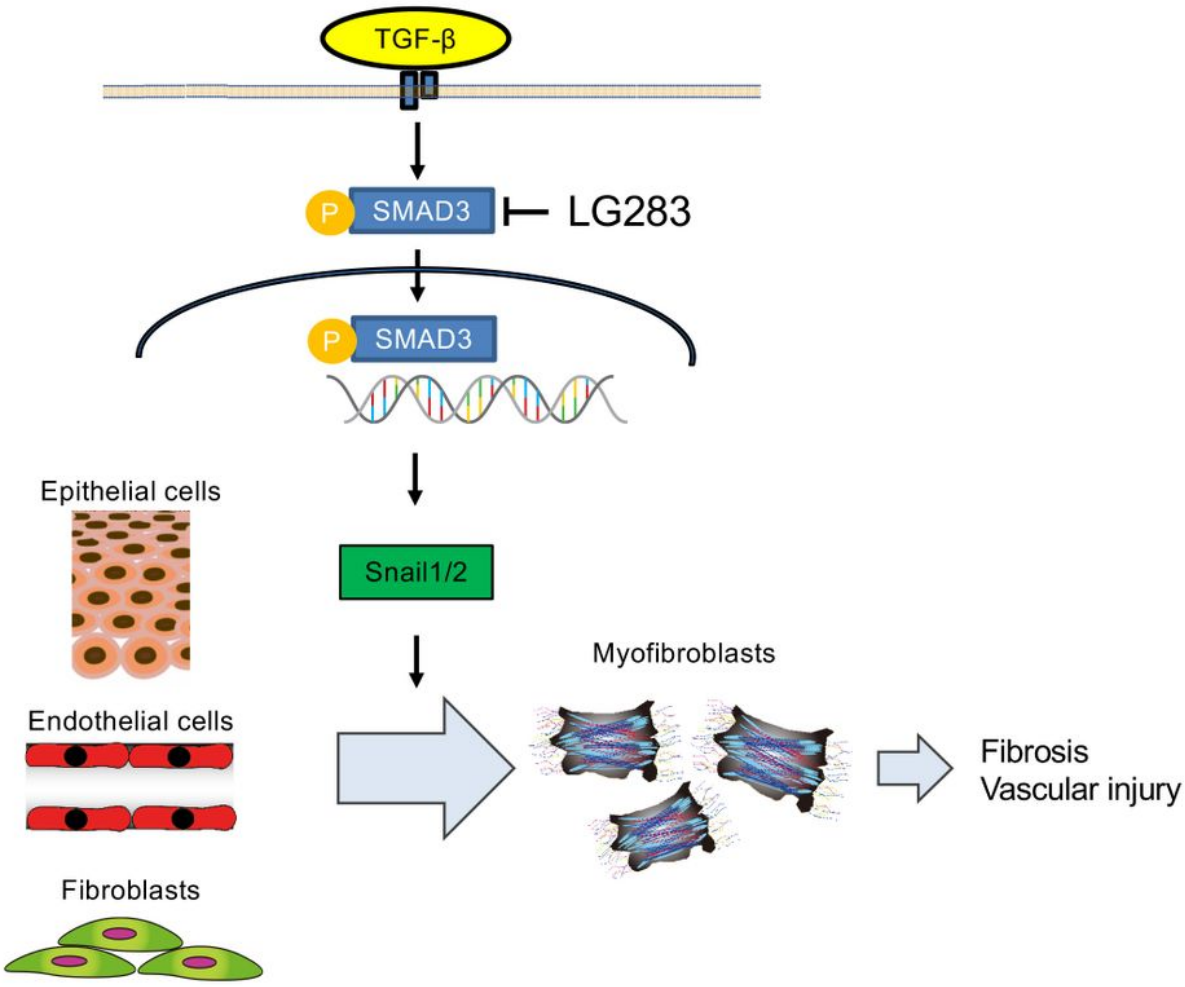

Figure 8

Putative mechanism of LG283-mediated inhibition of skin fibrosis.